

Plastic Buckling Simulation of Tubular Structures by Finite Element Limit Analysis

Hoon Huh and Hyun-Sup Kim

Department of Mechanical Engineering,
Korea Advanced Institute of Science and Technology
373-1 Kusong-dong Yusong-gu, Taejon, 305-701, Korea

ABSTRACT — This paper is concerned with numerical simulation of plastic modes of tubular structures. The simulation incorporates with finite element limit analysis based on the upper bound method and the minimization technique. The analysis considers sequential deformation of structures with work-hardening effects. The simulation results demonstrate plastic buckling is one of the collapse modes and occurs when the buckling load is smaller than other collapse loads in order for the plastic dissipation energy to be minimized.

I. INTRODUCTION

Plastic buckling has been conventionally studied with the bifurcation criterion elaborated by Hill [1959], Sewell [1963], Hutchinson [1974], and many other researchers. Hill placed the bifurcation criterion for elasto-plastic solids on a firm mathematical foundation, which embraces solids characterized by smooth or cornered yield surfaces. The bifurcation theory, however, has many restrictions in application of complicated structures, which are usually analyzed by a simple bifurcation model.

Square and cylindrical tubes are widely used as structural members since they can be produced with various thickness/width ratios. Its axial collapse modes can be characterized according to the width/thickness ratio (Mahmood and Paluszny [1981]). Experimental data and approximate theoretical prediction for axial crushing with square and cylindrical tubes has been studied widely. The collapse analysis of square and cylindrical tubes has been focused on the determination of force-shortening characteristics and mean crushing force for the estimation of energy absorption efficiency. Mahmood and Paluszny [1981] proposed semi-empirical approach for the purpose of developing method to calculate the mean crush load and maximum load capacity of axially loaded thin-walled columns. Wierzbicki and Abramowicz [1983] proposed basic folding mechanism with

kinematic continuity on the boundaries between rigid and deformable zones, and showed that the proposed theory can predict the mean crushing force and the associated collapse mechanism for axially compressed rectangular box columns. Abramowicz and Jones [1986] performed an experimental validation of the theory. Since empirical method usually depends on experiments and theoretical prediction, it is difficult to account the hardening effect of the material and describe the detail deformation mode. To avoid unrealistic buckling mode, strain hardening is an important factor which can not be neglected for the plastic buckling analysis of tubular structures even if the degree of hardening is small (Li and Reid [1992]).

Limit analysis has advantage of dealing with any type of plastic deformation, bounding the collapse load by the upper limit and lower limit. Finite element limit analysis has more capability to calculate the collapse load and the collapse mode of complicated structures without any prior conjectures. The solution process of finite element limit analysis minimizes the dual functional of the plastic dissipation energy (Huh et al. [1991]). When the minimization of the dual functional needs a bifurcation mode, the analysis automatically produces a bifurcation mode as well as the collapse load in the sense of load-carrying capacity. Huh and Lee [1993] suggested method to consider the work-hardening effect in the finite element limit analysis. The method extended from the conventional limit analysis makes it possible to simulate the collapse behavior of three-dimensional structures with work-hardening materials using finite element limit analysis (Kim and Huh [1999]).

In this paper, plastic buckling of cylindrical and square tubes has been successfully simulated by finite element limit analysis. The present analysis is concerned with the collapse behavior of tubular structures under the quasi-static loading condition as analysis for the estimation of load-carrying capacity and energy absorption efficiency. The finite element limit analysis code, used in this paper, considers sequential deformation of structures with work-hardening effects. A comparison of the experiments with finite element limit analysis results showed good agreement in collapse load and collapse mode. And the results demonstrate that the present analysis can predict weak parts of the structure automatically of the type of deformation.

II. LIMIT ANALYSIS THEORY

The limit analysis formulation consists of the primal and dual formulations. It addresses plastic materials which obey the convex yield criterion and the associated flow rule. The primal formulation can be derived from the statically and constitutively admissible conditions in the form of a constrained maximization problem, i.e.,

$$\begin{aligned}
 & \text{maximize } q(\boldsymbol{\sigma}) \\
 & \text{subject to } \nabla \cdot \boldsymbol{\sigma} = 0 \text{ in } D \\
 & \quad \boldsymbol{\sigma} \cdot \mathbf{n} = q\mathbf{t} \text{ on } \partial D_s \\
 & \quad \|\boldsymbol{\sigma}\|_{(v)} \leq \sigma_o \text{ in } D
 \end{aligned} \tag{1}$$

where $\boldsymbol{\sigma}$ is the stress tensor in the reference domain D , \mathbf{t} is a traction force vector on the boundary surface ∂D_s whose unit outer normal vector is \mathbf{n} , and q is a positive real parameter of proportional loading. The statically admissible set in the stress space can be formed with the state of stress that satisfies the equation of equilibrium and the static boundary conditions. The von-Mises yield criterion $\|\boldsymbol{\sigma}\|_{(v)} = \sigma_o$ is regarded as the constitutively admissible set. Although q can be uniquely obtained in Eqn. (1), $\boldsymbol{\sigma}$ may or may not be unique.

Eqn. (1) defines a convex surface in the function space $R^{3 \times 3}(D)$ and seeks the maximum of the positive scaling factor $q(\boldsymbol{\sigma})$, while the magnitude of the stress matrix, $\boldsymbol{\sigma}$, is constrained by the von-Mises yield condition in the convex norm. While this kind of maximization problem, the lower bound formulation in plasticity, can be solved by finite dimensional approximation, it is not practical and efficient since the solution needs to be determined in a stress space.

The convex problem has a dual one which corresponds to the upper bound formulation. The minimum solution of dual formulation is equal to the maximum $q(\boldsymbol{\sigma})$ in Eqn. (1). To construct the dual problem, the principle of virtual work is used to form a weak equilibrium equation,

$$\int_D \mathbf{u} \cdot (\nabla \cdot \boldsymbol{\sigma}) \, d\Omega = 0 \quad , \forall \mathbf{u} \tag{2}$$

where \mathbf{u} is an arbitrary function in $\mathbb{R}^3(D)$ with the physical interpretation as an admissible velocity function. The above integration is carried out in the reference domain of two or three dimension for each incremental step. The admissible \mathbf{u} , which satisfies the kinematic boundary conditions on ∂D_k , will lead to the equivalent variational statement, by applying the divergence theorem and static boundary conditions,

$$\int_D \boldsymbol{\sigma} : \boldsymbol{\varepsilon} \, d\Omega = q \int_{\partial D_s} \mathbf{t} \cdot \mathbf{u} \, d\Gamma \quad (3)$$

where $\boldsymbol{\varepsilon}$ is the strain rate matrix and the symbol $:$ denotes the inner product operator between two matrices. Eqn. (3) can be restated in an alternative way as follows

$$q(\boldsymbol{\sigma}) = \int_D \boldsymbol{\sigma} : \boldsymbol{\varepsilon} \, d\Omega = \int_D \sigma_{ij} \varepsilon_{ij} \, d\Omega \quad (4)$$

where the boundary integral in Eqn. (3) has been normalized, i.e.,

$$\int_{\partial D_s} \mathbf{t} \cdot \mathbf{u} \, d\Gamma = 1 \quad (5)$$

Using the principle of maximum work dissipation or by a generalized Hölder inequality, the term $\boldsymbol{\sigma} : \boldsymbol{\varepsilon}$ can be rewritten as follows,

$$\boldsymbol{\sigma} : \boldsymbol{\varepsilon} = \boldsymbol{\sigma} : \boldsymbol{\varepsilon} \leq \|\boldsymbol{\sigma}\|_{(v)} \|\boldsymbol{\varepsilon}\|_{(-v)} = \bar{\sigma} \bar{\varepsilon} \quad (6)$$

where $\|\boldsymbol{\sigma}\|_{(v)}$ denotes the von-Mises norm of the stress, and $\|\boldsymbol{\varepsilon}\|_{(-v)}$ denotes the minus von-Mises norm of the strain rate, which define the equivalent stress and strain rate, respectively.

The inequality is sharp, i.e., the equality holds when $\boldsymbol{\varepsilon}$ is chosen to be proportional to the gradient of the yield function. The sharpness condition

$$\boldsymbol{\varepsilon} = k \|\boldsymbol{\sigma}\|_{(v)} \quad (7)$$

is the well known normality condition in plasticity, where k is a proportional factor. Consequently, an upper bound to the functional, $q(\boldsymbol{\sigma})$, can be established through the sequence of inequalities as

$$\begin{aligned}
q(\boldsymbol{\sigma}) &= \int_D \boldsymbol{\sigma} : \boldsymbol{\varepsilon} \, d\Omega \\
&\leq \int_D \|\boldsymbol{\sigma}\|_{(v)} \|\boldsymbol{\varepsilon}\|_{(-v)} \, d\Omega \\
&\leq \sigma_o \int_D \|\boldsymbol{\varepsilon}\|_{(-v)} \, d\Omega \\
&= \tilde{q}(\mathbf{u})
\end{aligned} \tag{8}$$

where the upper bound functional $\tilde{q}(\mathbf{u})$ depends only on the kinematically admissible function \mathbf{u} . Based on the inequality in Eqn. (8) and the existence of the absolute minimum of $\tilde{q}(\mathbf{u})$, the dual formulation may be stated as

$$\begin{aligned}
&\text{minimize } \tilde{q}(\mathbf{u}) \\
&\text{subject to } \tilde{q}(\mathbf{u}) = \sigma_o \int_D \|\boldsymbol{\varepsilon}\|_{(-v)} \, d\Omega \\
&\int_{\partial D_s} \mathbf{t} \cdot \mathbf{u} \, d\Gamma = 1 \\
&\text{Tr}(\boldsymbol{\varepsilon}) = 0 \\
&\text{Kinematic boundary conditions}
\end{aligned} \tag{9}$$

The minimum solution of $\tilde{q}(\mathbf{u})$ is equal to the maximum $q(\boldsymbol{\sigma})$ in formulation (1), within the smallest part of the kinematically admissible function spaces, by the duality relation (Huh and Yang, 1991). In real problems, a general solution of formulation (9) could be obtained using numerical methods.

In the calculation for work-hardening materials, the effective stress–strain curve is considered as step-wise constant, but the magnitude of the current yield stress, σ_o , is adjusted based on the effective strain by successive iterations using the bisection method (Huh and Lee, 1993, 1998), i.e.,

$$\sigma_o = \bar{\sigma} = F(W_p) \text{ or } H(\bar{\varepsilon}^p) \tag{10}$$

where $F(W_p)$ and $H(\bar{\varepsilon}^p)$ represent functions for work-hardening and strain-hardening, respectively, and $\bar{\varepsilon}^p$

indicates the equivalent plastic strain. Considering the current yield stress in each incremental step, there is no need to check whether the stress–strain relation is correctly tracking the given data due to the nature of the formulation. The above concept extended from the conventional limit analysis makes it possible to simulate the collapse behavior of three-dimensional structures with work-hardening materials by using finite element limit analysis. Although there might be a small amount of error with the assumption that the current yield stress is considered as a constant, it ensures stable convergence and computational efficiency even in shakedown. It also removes the accumulated error that often comes from the calculation of plastic or elasto-plastic tangent modulus in each incremental step. The amount of increment should allow that the maximum effective strain in each step is less than 0.2%. The current yield stress can be obtained from a typical uniaxial stress–strain relation

$$\bar{\sigma} = \sigma_o \left(1 + A \bar{\varepsilon}^p \right)^n \quad (11)$$

where A and n are the constants for a given material, and σ_o is the initial yield stress.

III. FINITE ELEMENT PROCEDURES AND MINIMIZATION TECHNIQUE

The dual formulation is discretized into the sub-domains of finite elements and reduced to a convex problem in the finite dimensional space \mathbb{R}^N , where N is the total number of discrete variables. To guarantee the incompressibility condition, the objective functional is modified as

$$\tilde{q}(\mathbf{u}) = \bar{\sigma} \int_D \|\boldsymbol{\varepsilon}\|_{(-\nu)} d\Omega + \Lambda \int_D u_{i,i}^2 d\Omega \quad (12)$$

where Λ is a penalty factor which can be a large number.

For the finite dimensional approximation, the strain rate vector in a three-dimensional space can be expressed in a matrix form as

$$\boldsymbol{\varepsilon} = \left\{ \varepsilon_x \ \varepsilon_y \ \varepsilon_z \ \sqrt{2}\varepsilon_{xy} \ \sqrt{2}\varepsilon_{yz} \ \sqrt{2}\varepsilon_{zx} \right\}^T = \mathbf{B}\mathbf{U} \quad (13)$$

where \mathbf{B} is the gradient matrix related to the strain rate components and \mathbf{U} is the nodal velocity vector. Then, the effective strain rate can be written as

$$\bar{\varepsilon} = \sqrt{\frac{2}{3} \varepsilon_i \varepsilon_i} = \sqrt{\frac{2}{3} \mathbf{U}^T \mathbf{B}^T \mathbf{B} \mathbf{U}} = \sqrt{\mathbf{U}^T \mathbf{K}_1 \mathbf{U}} \quad (14)$$

where $\mathbf{K}_1^e = \frac{2}{3} \mathbf{B}^T \mathbf{B}$. The matrix form of volumetric strain rate can be written as

$$\begin{aligned} \varepsilon_v &= \varepsilon_x + \varepsilon_y + \varepsilon_z \\ &= \{1 \ 1 \ 1 \ 0 \ 0 \ 0\} \left\{ \varepsilon_x \ \varepsilon_y \ \varepsilon_z \ \sqrt{2} \varepsilon_{xy} \ \sqrt{2} \varepsilon_{yz} \ \sqrt{2} \varepsilon_{zx} \right\}^T \\ &= \mathbf{A} \mathbf{B} \mathbf{U} = \mathbf{K}_2 \mathbf{U} \end{aligned} \quad (15)$$

where \mathbf{A} is a vector, $\{1 \ 1 \ 1 \ 0 \ 0 \ 0\}$ and $\mathbf{K}_2 = \mathbf{A} \mathbf{B}$.

The objective functional is approximated using finite elements in a quadratic form of the discrete vector representation of the velocity field, \mathbf{U} , i.e.,

$$\tilde{q}(\mathbf{U}) = \sum_{e=1}^E \left[\mathbf{U}^T \hat{\mathbf{K}}_1^e \mathbf{U} + \mathbf{U}^T \hat{\mathbf{K}}_2^e \mathbf{U} \right] \quad (16)$$

where the integer E is the total number of the finite elements, and

$$\hat{\mathbf{K}}_1^e = \bar{\sigma} \int_{D_e} \frac{\mathbf{K}_1^e}{\sqrt{\mathbf{U}^T \mathbf{K}_1^e \mathbf{U}}} d\Omega \quad (17)$$

$$\hat{\mathbf{K}}_2^e = \Lambda \int_{D_e} \mathbf{K}_2^{eT} \mathbf{K}_2^e d\Omega$$

The element stiffness matrix in Eqn. (17) can be approximated as follows for an iterative scheme

$$\left(\hat{\mathbf{K}}_1^e\right)_n = \bar{\sigma} \int_{D_e} \frac{\left(\mathbf{K}_1^e\right)_n}{\sqrt{\left(\mathbf{U}^T \mathbf{K}_1^e \mathbf{U}\right)_{n-1}}} d\Omega \quad (18)$$

where $(n-1)$ and (n) indicate the previous iterative step and current step, respectively.

The approximation of the dual formulation (9) becomes a constrained quadratic problem, i.e.,

$$\begin{aligned} & \text{minimize } \tilde{q}(\mathbf{U}) = \mathbf{U}^T \mathbf{K} \mathbf{U} \\ & \text{subject to } \mathbf{C}^T \mathbf{U} = 1 \end{aligned} \quad (19)$$

where $\mathbf{C}^T \mathbf{U} = 1$ represents the normality condition and the kinematic boundary conditions are absorbed into the matrix \mathbf{K} and vector \mathbf{C} which will yield the optimum \mathbf{U}_n and the minimum value q_n associated for each iterative step. The constrained minimization formulation (19) is converted to an unconstrained problem in the solution procedure with the use of the Lagrange multiplier method, i.e.,

$$\text{minimize } \Phi(\mathbf{U}) = \mathbf{U}^T \mathbf{K} \mathbf{U} - 2\lambda(\mathbf{C}^T \mathbf{U} - 1) \quad (20)$$

where λ is the Lagrange multiplier.

Differentiating Eqn. (20) with respect to the displacement and Lagrange multiplier results in the following equations:

$$\frac{\partial \Phi}{\partial \mathbf{U}} = 2\mathbf{K}\mathbf{U} - 2\lambda\mathbf{C} = 0 \quad (21)$$

$$\frac{\partial \Phi}{\partial \lambda} = \mathbf{C}^T \mathbf{U} - 1 = 0 \quad (22)$$

From Eqn. (21) and (22), following equation can be obtained

$$\mathbf{U} = \lambda \mathbf{K}^{-1} \mathbf{C} \quad (23)$$

$$\lambda = \mathbf{U}^T \mathbf{K} \mathbf{U} \quad (24)$$

or

$$\lambda = \frac{1}{\mathbf{C}^T \mathbf{K}^{-1} \mathbf{C}} \quad (25)$$

When the displacement boundary condition is given, the displacement vector can be divided into two parts as

$$\mathbf{U} = \begin{Bmatrix} \mathbf{U}_1 \\ \mathbf{U}_2 \end{Bmatrix} \quad (26)$$

where $\{\mathbf{U}_1\}$ is an unknown displacement vector and $\{\mathbf{U}_2\}$ is known from the boundary condition. The stiffness matrix \mathbf{K} also can be divided into sub-matrices corresponding to the given displacement boundary condition as

$$\mathbf{K} = \begin{bmatrix} \mathbf{K}_{11} & \mathbf{K}_{12} \\ \mathbf{K}_{21} & \mathbf{K}_{22} \end{bmatrix} \quad (27)$$

The load vector also can be divided into two parts as

$$\mathbf{C} = \begin{Bmatrix} \mathbf{C}_1 \\ \mathbf{C}_2 \end{Bmatrix} \quad (28)$$

where $\{\mathbf{C}_1\}$ becomes zero when only the displacement boundary condition is given and $\{\mathbf{C}_2\}$ is unknown at the region where the displacement boundary condition is given. Using the partitioned stiffness matrices and displacement vectors, Eqn. (21) can be restated as

$$\begin{bmatrix} \mathbf{K}_{11} & \mathbf{K}_{12} \\ \mathbf{K}_{21} & \mathbf{K}_{22} \end{bmatrix} \begin{Bmatrix} \mathbf{U}_1 \\ \mathbf{U}_2 \end{Bmatrix} = \lambda \begin{Bmatrix} \mathbf{C}_1 \\ \mathbf{C}_2 \end{Bmatrix} \quad (29)$$

Eqn. (29) can be divided into two independent sets of equations as

$$[\mathbf{K}_{11}]\{U_1\} + [\mathbf{K}_{12}]\{U_2\} = \lambda\{C_1\} = \{0\} \quad (30)$$

$$[\mathbf{K}_{21}]\{U_1\} + [\mathbf{K}_{22}]\{U_2\} = \lambda\{C_2\} \quad (31)$$

From the Eqn. (30), $\{U_1\}$ can be obtained as

$$\{U_1\} = -[\mathbf{K}_{11}]^{-1}([\mathbf{K}_{12}]\{U_2\}) \quad (32)$$

and then the displacement vector is restated as

$$U = \begin{Bmatrix} -[\mathbf{K}_{11}]^{-1}([\mathbf{K}_{12}]\{U_2\}) \\ U_2 \end{Bmatrix} \quad (33)$$

Using the vector $\{U_1\}$ obtained from Eqn. (32), $\lambda\{C_2\}$ can be calculated using Eqn. (31) and the vector λC is restated as

$$\lambda C = \begin{Bmatrix} 0 \\ [\mathbf{K}_{21}]\{U_1\} + [\mathbf{K}_{22}]\{U_2\} \end{Bmatrix} \quad (34)$$

Then, the solution of the problem may then be expressed symbolically as

$$U_n = \lambda K^{-1} C = \frac{K^{-1} C}{C^T K^{-1} C} \quad (35)$$

$$\tilde{q}_n = U^T K U = \left(\frac{K^{-1} C}{C^T K^{-1} C} \right)^T K \left(\frac{K^{-1} C}{C^T K^{-1} C} \right) = \lambda_n \quad (36)$$

for the n -th iteration step. The iteration results from Eqn. (35) and (36) are used in a feed-back loop to update K

and λ . The iteration will be terminated when the following convergence criterion is satisfied

$$\frac{\|U_n - U_{n-1}\|}{\|U_n\|} \leq \delta_1 \quad (37)$$

$$\frac{\|\tilde{q}_n - \tilde{q}_{n-1}\|}{\|\tilde{q}_n\|} \leq \delta_2 \quad (38)$$

where δ_1 and δ_2 represent the desired accuracy of the solution.

REFERENCES

- 1959 Hill, R. J. *Mech. Phys. Solids*, **7**, 209.
- 1963 Sewell, M. J., *J. Mech. Phys. Solids*, **11**, 377.
- 1974 Hutchinson, J. W., in *Advances in Applied Mechanics*, Vol. 14, pp. 67-144, Academic Press, New York.
- 1981 Mahmood, H. F. and Paluszny, A., "Design of Thin Walled Columns for Crash Energy Management—Their Strength and Mode of Collapse," SAE, **811302**, 4039.
- 1983 Wierzbicki, T. and Abramowicz, W., "On the crushing mechanics of thin-walled structures," *ASME J. Appl. Mech*, **50**, 727.
- 1986 Abramowicz, W., and Jones, N., "Dynamic progressive buckling of circular and square tubes," *Int. J. Impact Engineering*, **4**, No. 4, 243.
- 1992 Li, S. and Reid, S. R., "The Plastic Buckling of Axially Compressed Square Tubes," *Trans. ASME J. Appl. Mech.*, **59**, 276.
- 1991 Huh, H. and Yang, W. H., "A General Algorithm for Limit Solutions for Plane Stress Problems," *Int. J. Solids Struct.*, **28**, **6**, 727.
- 1993 Huh, H. and Lee, C. H., "Eulerian Finite Element Modeling of the Extrusion Process for Work-hardening Materials with the Extended Concept of Limit Analysis," *J. Mat. Proc. Tech.*, **5**, 51.
- 1999 Kim, H. S. and Huh, H., "Vehicle Structural Collapse Analysis using a Finite Element Limit Method, *International Journal of Vehicle Design*," *Int. J. Veh. Des.*, **21**, **4/5**, (in print).
- 1998 Huh, H. et al., "," *Int. J. Solids Struct.*, **35**, **10**, (in print).
- 1977 Johnson, W. et al., *J. Strain Anal.*, **12**, **4**, 317.



Fig. Deformed shape of a cylindrical tube ($D : H = 1 : 1$)



Fig. Deformed shape of a cylindrical tube ($D : H = 1 : 2$)

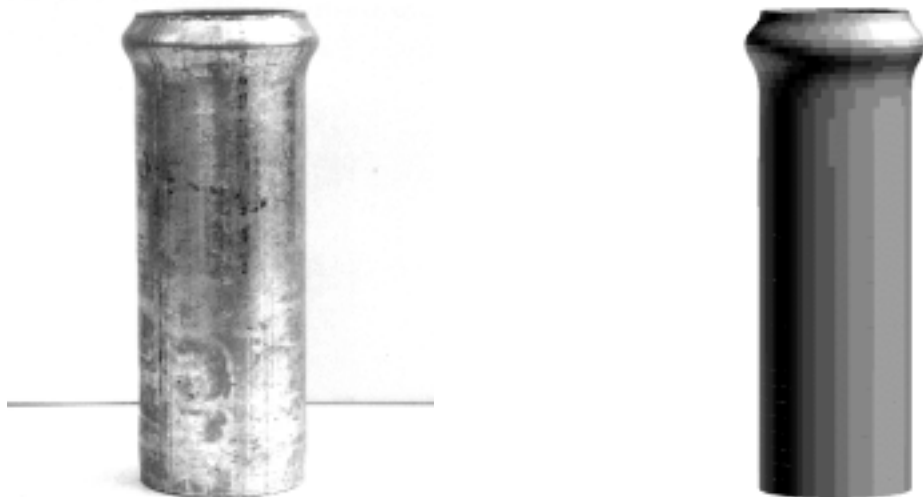


Fig. Deformed shape of a cylindrical tube ($D : H = 1 : 3$)

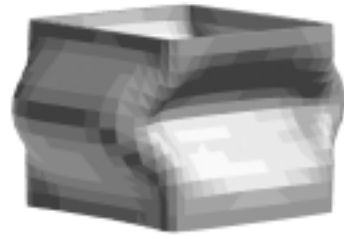


Fig. Deformed shape of a square tube ($L : H = 1 : 1$)



Fig. Deformed shape of a square tube ($L : H = 1 : 2$)



Fig. Deformed shape of a square tube ($L : H = 1 : 3$)



Fig. Deformed shape of a square tube extensional mode ($L : H = 1 : 2$)

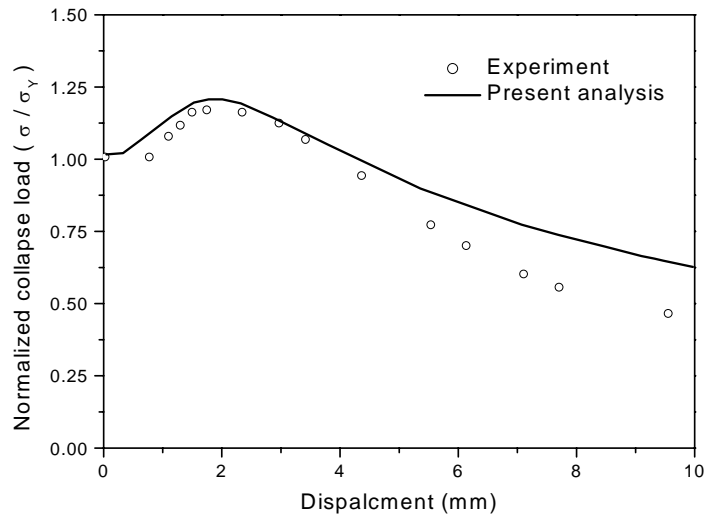


Fig. Collapse load with respect to axial displacement of a cylindrical tube (D : H = 1: 1)

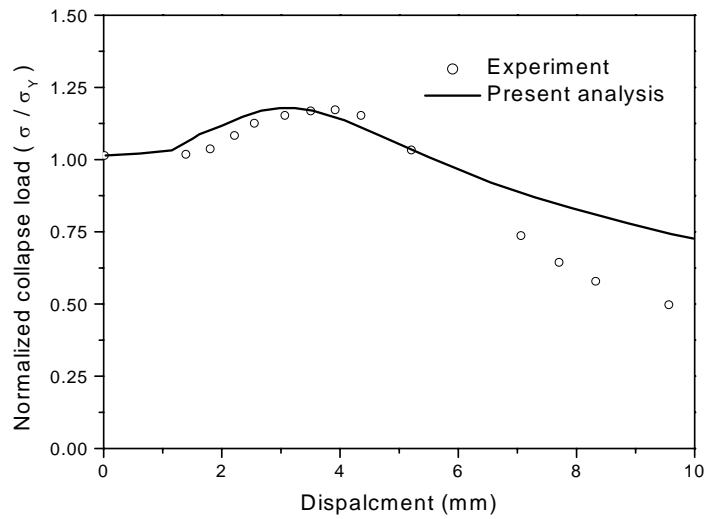


Fig. Collapse load with respect to axial displacement of a cylindrical tube (D : H = 1: 2)

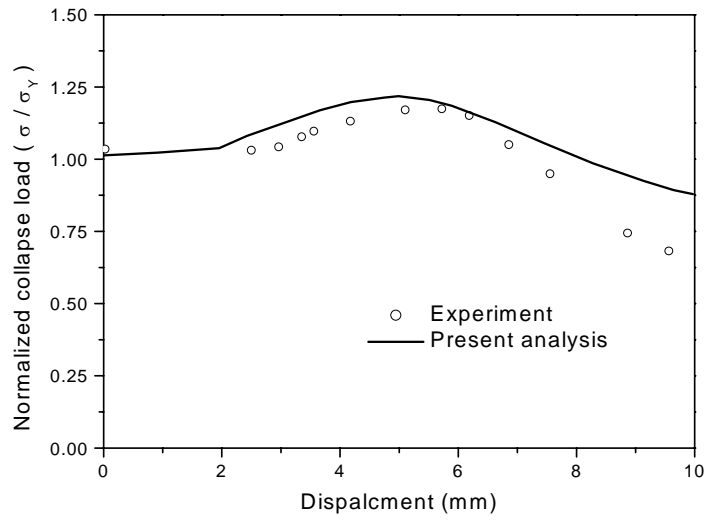


Fig. Collapse load with respect to axial displacement of a cylindrical tube (D : H = 1 : 3)

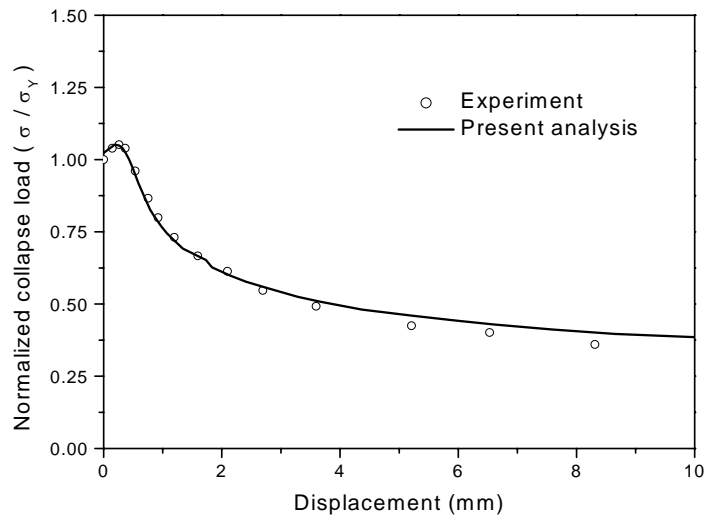


Fig. Collapse load with respect to axial displacement of a square tube (L : H = 1 : 1)

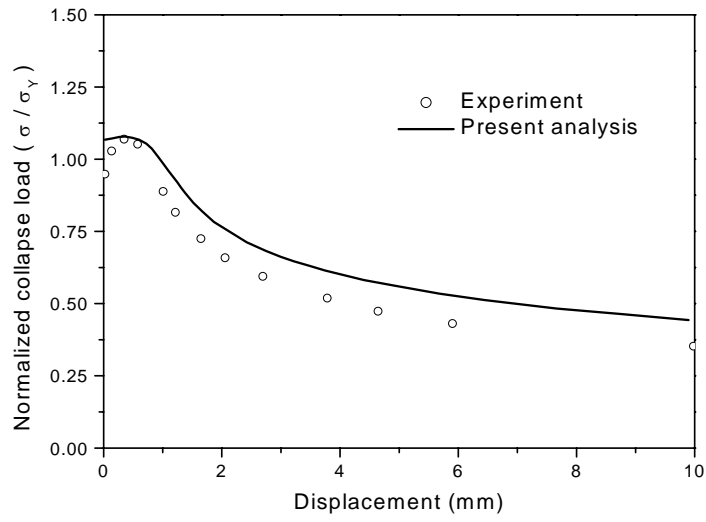


Fig. Collapse load with respect to axial displacement of a square tube (L : H = 1 : 2)

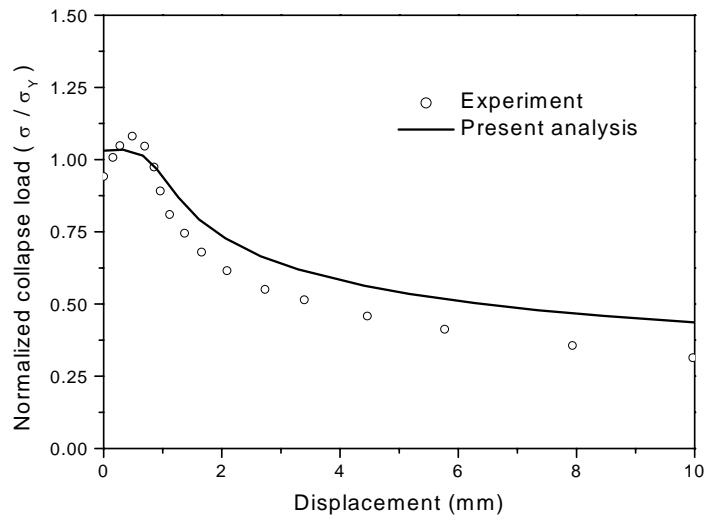


Fig. Collapse load with respect to axial displacement of a square tube (L : H = 1 : 3)

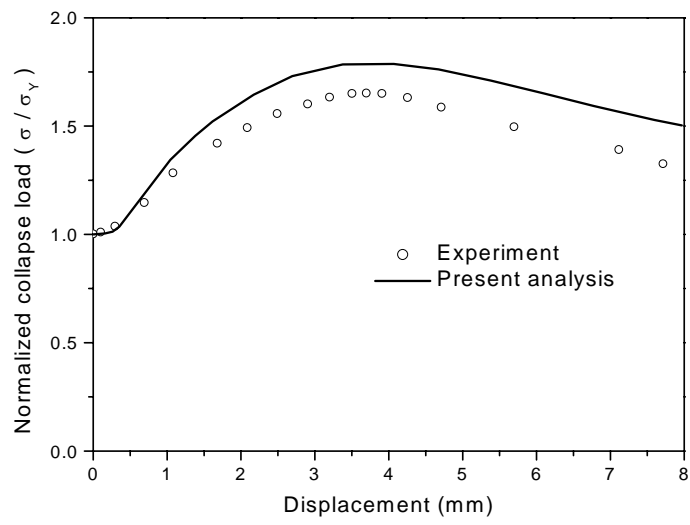


Fig. Collapse load with respect to axial displacement of a square tube extensional mode ($L : H = 1 : 2$)